

Imaging Alzheimer's: In Vivo Detection of β -Amyloid Deposits by Near-Infrared Imaging

H.-U. Gremlich, Ph.D., M. Hintersteiner, Ph.D.,
R. Kneuer, Ph.D., M. Stoeckli, Ph.D., A. Suter
Discovery Technologies
Novartis Institutes for Biomedical Research Basel,
Switzerland

As Alzheimer's disease pathogenesis is associated with the formation of insoluble aggregates of amyloid- β peptide, approaches allowing the direct, noninvasive visualization of plaque growth in vivo would be beneficial for biomedical research. This is a description of the in vivo imaging application of the in-house synthesized first plaque-specific near-infrared fluorescence dye (AOI987), which readily penetrates the intact blood-brain barrier and binds to β -amyloid plaques. Using near-infrared fluorescence imaging, specific interaction of the oxazine dye AOI987 with amyloid plaques in APP23

transgenic mice has been demonstrated in vivo as confirmed by postmortem analysis of brain slices. Quantitative analysis revealed increasing fluorescence signal intensity with increasing plaque load of the animals and significant binding of AOI987 was observed for APP23 transgenic mice of age 9 months and older. Thus, the plaque-specific dye AOI987 is an attractive probe to noninvasively monitor disease progression in animals of Alzheimer's disease and to evaluate effects of potential Alzheimer's disease drugs on the plaque load.

Introduction

The clinical characteristics of Alzheimer's disease (AD) are dementia, cognitive impairment, and memory loss. On a histological level, the accumulation and deposition of amyloid- β (A β) peptides A β 1-40 and A β 1-42 into amyloid plaques (AP) is considered an important hallmark in AD pathogenesis [1, 2]. These A β peptides result from cleavage of amyloid precursor protein (APP) by proteases called β - and γ -secretases. Another pathomorphological hallmark of AD are neurofibrillary tangles (NFT) composed of the hyperphosphorylated microtubule-associated protein tau [1, 2]. Today, clinical diagnosis of AD is based on mental and cognitive examinations of patients [3], and definitive confirmation of AD is obtained only postmortem by histopathological examination of brain tissue for APs and NFTs. Therefore, approaches allowing the direct visualization of the growth of the AP load (and NFTs) in vivo would be beneficial for the assessment of the disease status.

Imaging of APs using structural imaging techniques, such as magnetic resonance imaging (MRI), has to face the high demands on spatial resolution required for the identification of individual plaques (diameter $\leq 50 \mu\text{m}$). While feasible in fixed human brain specimen and in vivo in transgenic mouse models of AD, translation of these approaches to clinical use is not yet possible. In addition, the sensitivity of MRI is low due to a small specific contrast between plaques and surrounding tissue. Imaging of AP with high sensitivity, (i. e., high contrast between AP-associated signals and the background) critically depends on the development of contrast agents that specifically enhance AP signals. Such agents would be of high value for early diagnosis and monitoring of disease progression, as well as for the evaluation of therapeutic interventions. A number of promising candidate compounds have been described [4, 5]: plaque-specific ligands for positron emission tomography (PET), MRI, multiphoton microscopy, and optical imaging. Multiphoton microscopy is invasive, probes only small fields of view, and, hence, is of limited use for in vivo applications. Drawbacks of MRI-based approaches are low sensitivity and low blood-brain barrier (BBB) penetration of the bulky MRI ligands. For PET, limitations are the short half-life of positron-emitting nuclei and the limited availability of the technology, in particular for animal research. Nevertheless,

with regard to clinical application, PET currently seems to be the most promising approach [6]. An alternative imaging technology exploits the low absorption coefficients of light in the near-infrared (NIR) region of the electromagnetic spectrum. For wavelengths λ between 650 and 900 nm, light attenuation is typically one order of magnitude per 10 mm of tissue. With the availability of dyes that absorb and fluoresce in this spectral domain, near-infrared fluorescence (NIRF) imaging has evolved to a powerful and inexpensive tool for noninvasive imaging of target-specific interactions in animals [7]. We have synthesized and characterized the oxazine derivative AOI987 as first NIRF ligand with the properties required to target APs in vivo [5]. Administration of the dye to APP23 transgenic mice overexpressing human APP, which develop cerebral AP deposits starting at an age of six months, revealed specific binding to APs: the fluorescence intensity was significantly higher in APP23 mice compared to age-matched littermates. Moreover, quantitative image analysis demonstrated that the integrated fluorescence signal reflects the AP load of APP23 mice.

Methods

Chemical synthesis: The NIRF ligand AOI987 has been synthesized and characterized as described in [5].

Animal preparation: Female APP23 transgenic mice ($3 \leq n \leq 5$) and age-matched wild-type littermates ($2 \leq n \leq 4$) of age 6, 9, 10, 12, 14, 16, 17, and 21 months were used at around 25 g body weight. For NIRF experiments, the animals were anaesthetized using 1.5% Isoflurane (Abbott, Cham) in nitrous oxide/oxygen 2:1 administered via a face mask. The duration of anesthesia was 3 minutes. The dyes were administered intravenously (i.v.) into the tail vein at various doses (vehicle 0.9% saline, injection volume 10 ml/kg). NIRF images were recorded 30, 60, 120, and 240 minutes after dye administration. To avoid problems caused by light scattering due to the fur, animals were shaved for the NIRF experiments. In order to determine the optimal dose, various doses of AOI987 were administered i.v. (3, 1, 0.3, 0.1, and 0.01 mg/kg) to female APP23 transgenic and nontransgenic mice. Four hours after probe application, the difference of the normalized signal intensities I_{rel} between transgenic and nontransgenic mice was highest for a dosage of 0.1 mg/kg. The dye was completely washed out 24 hours

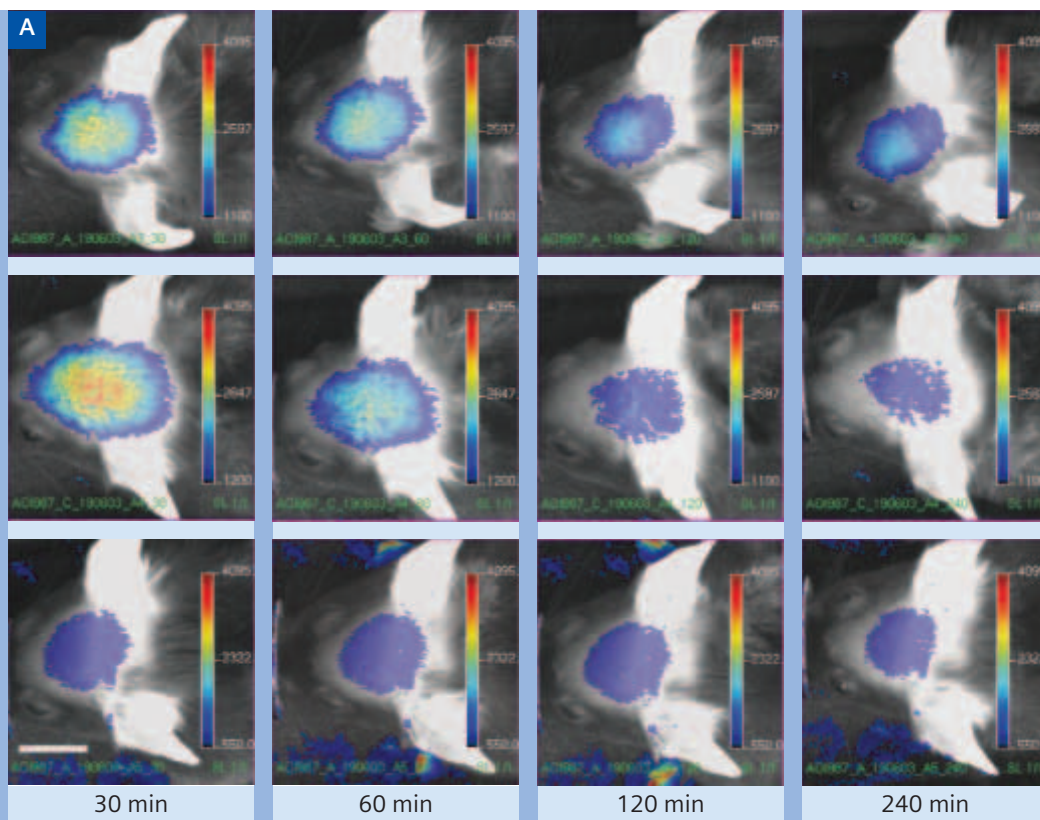
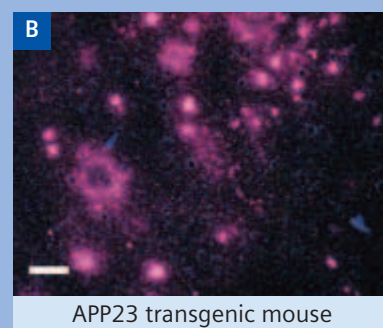


(Figure 1)

[A] *In vivo* imaging of amyloid- β deposits: Representative images of female 17-month-old APP23 transgenic (top row) and wild-type (middle row) mice, injected i.v. with 0.1 mg/kg AOI987. The images were recorded 30, 60, 120, and 240 minutes after the injection of the fluorescent dye. In the bottom row, corresponding images of a female 17-month-old transgenic APP23 mouse treated with 0.9% saline only are shown. Scale bar 1 cm; color scale bars arbitrary units.

[B] NIR Fluorescence microscopy of air-dried cryotome sections (20 μ m thickness) of 16-month-old female mice that have been dosed with 0.1 mg/kg AOI987 i.v. The brains were excised and fixed 4 hours following dye administration; APP23 transgenic.



APP23 transgenic mouse

after i.v. application. Uptake of AOI987 in peripheral organs has been found; yet no acute toxicity was observed at any of the doses used.

NIRF imaging: In vivo NIRF imaging was carried out using a 'bonSAI' small animal imager prototype (Siemens AG, Medical Solutions, Erlangen, Germany). For fluorescence excitation, three light-emitting diodes at 660 nm with a total power of 10 mW/cm² were used, yielding a uniform illumination of the whole animal. The fluorescent light emitted from the sample (mouse) was detected by a charge-coupled device (CCD) camera (Hamamatsu ORCA) equipped with a focusing lens system (macro lens 60 mm, 1:2.8, Nikon). The image matrix comprised 532 x 256 pixels. A bandpass filter was used for the selection of the detection wavelength (700 nm). Data collection (i.e., integration times) ranged from 0.5 to 3.0 seconds depending on the fluorescence intensity. The experiment was controlled by a PC using the Siemens *syngo*[®] software. NIRF images have been evaluated quantitatively using region-of-interest analysis tools provided by BioMap 3.05, an in-house-developed image analysis software tool (<http://www.maldi-msi.org>). Autofluorescence measured immediately prior to dye administration turned out to be negligible. All experiments were carried out in adherence to the Swiss laws of animal protection.

Results

In vivo NIRF imaging: After BBB penetration of the oxazine dye AOI987 had been affirmed [5], female 17-month-old APP23 transgenic mice (n = 3 to 5) and age-matched wild-type littermates (n = 2 to 4) were used to assess the potential of AOI987 for specific AP imaging in vivo using NIRF imaging. Various amounts of the dyes (0.1, 1, and 3 mg/kg; vehicle 0.9% saline) were injected i.v. into the tail vein. Immediately after dosing an intense fluorescence signal could be detected in the brain. The disappearance of the fluorescence signal was significantly slower in transgenic APP23 compared to wild-type animals. This is illustrated in Figure 1A by images recorded 30, 60, 120, and 240 minutes after i.v. injection with the previously established optimal dose of 0.1 mg/kg AOI987. The temporal behavior of the fluorescence signals was observed to be equal in 6-month-old APP23 transgenic and wild-type mice: histological analysis revealed a minimal AP load in these young animals. It was only at the age of

9 month that differences between APP23 transgenic and age-matched wild-type littermates became obvious. APP23 mice treated with the vehicle 0.9% saline showed solely background fluorescence at all time points (Figure 1A).

In vivo results were confirmed by ex vivo measurements on brains prepared 4 hours after dye administration, immediately after acquiring the final in vivo NIRF image. Fluorescence microscopy demonstrated selective in vivo staining of APs with AOI987 in APP23 mice, while the brain sections of wild-type animals showed no fluorescence signal (Figure 1B).

In order to exclude the possibility that the different temporal behavior of fluorescence signals might be due to altered dye metabolism/elimination in APP23 mice compared to nontransgenic littermate controls, we compared the time course of fluorescence signals originating from brains and thoraxes of 16-month-old female transgenic and wild-type mice. Following i.v. administration of AOI987 (0.1 mg/kg), identical rates of signal disappearance were observed for the thoracic regions of APP23 and control mice as well as for the brains of wild-type mice. However, brain signals of APP23 animals decreased at a significantly slower rate (Figure 2), which is indicative of specific dye retention in cerebral tissue of transgenic mice.

Quantification of in vivo NIRF imaging

Semiquantitative information was derived from NIRF images by normalizing the fluorescence intensity to that of the first measurement point, recorded 30 minutes after dye administration (I_{ref} , Figure 3A). Statistically significant differences between transgenic and wild-type mice were obtained at the 120-minute as well as at the 240-minute point ($P = < 0.001$, one-way ANOVA). The relative intensity parameter ($I_{rel}^{rel}(t) = I_{rel}(t) / I_{ref}$) displayed remarkable reproducibility, with coefficients of variation of 7% (3 measurements within 11 days with four 14-month-old female APP23 transgenic mice, measurement at 240 minutes after i.v. administration of 0.1 mg/kg AOI987).

The comparison of the fluorescence intensities observed in APP23 and wild-type mice provided a measure for the specific binding of AOI987 to APs as shown for 16-month-old transgenic APP23 mice that are injected

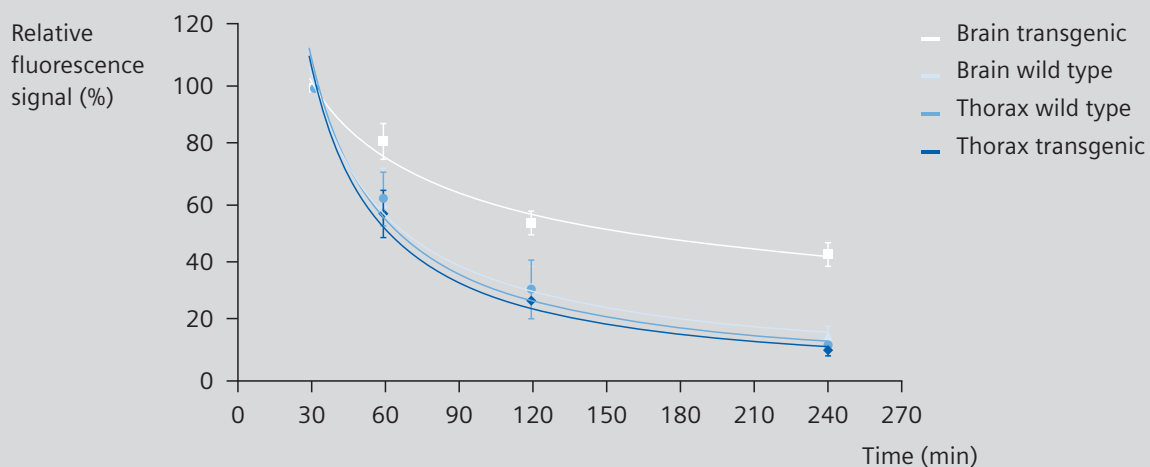


(Figure 2)

Time course of fluorescence signals originating from brain and thorax of 16-month-old female APP23 transgenic and wild type mice.

i.v. with 0.1 mg/kg AOI987 (Figure 3B). In results shown here, we define specific binding as the difference of the fluorescence signal of transgenic mice minus the fluorescence signal of nontransgenic mice divided by the fluorescence signal of transgenic mice, thereby accounting for unspecifically bound dye reaction.

The sensitivity of the in vivo assessment of the AP load using AOI987 as plaque-specific dye (dose 0.1 mg/kg, i.v.) was evaluated in a serial study involving female APP23 mice of different ages (Figure 3C). The fluorescence intensity increased with age as expected based on the well-documented increase in the AP load with age in this animal model of AD (Figure 3C). Two parameters were used to assess the plaque load, the relative signal intensities I_{β}^{rel} (4 h) measured 4 hours after dosing and the area under the curve or rate of the clearance curves. For both parameters, the corresponding values for age-matched wild-type animals were subtracted to correct for unspecific binding. A sigmoid relationship between the NIRF measures and the age of the animals (i.e., plaque load) was found (Figure 3C).

Discussion

As the oxazine dye AOI987 readily penetrates the BBB, displays specific binding to amyloid plaques, and provides quantitative information on plaque levels in AD model mice, it fulfills all requirements for selective in vivo staining of A β plaques.

Experiments using NIRF imaging demonstrated that amyloid deposits could be observed in living APP23 mice with intact cranium and BBB following i.v. administration of AOI987 at doses ranging from 0.1 to 3 mg/kg. Good discrimination between specific and unspecific dye accumulation was observed 4 hours after dosing. Specific labeling of APs could be confirmed unambiguously by ex vivo analysis of thin sections of the frozen APP23 brains that were removed immediately after NIRF imaging. The colocalization of the AOI987 fluorescence with the silver-methinamine staining, as well as the lack of staining of other brain structures, demonstrated a specific interaction of the AOI987 with the AP. Biological tissue is a highly scattering medium; the diffuse nature of light propagation in tissue prevents

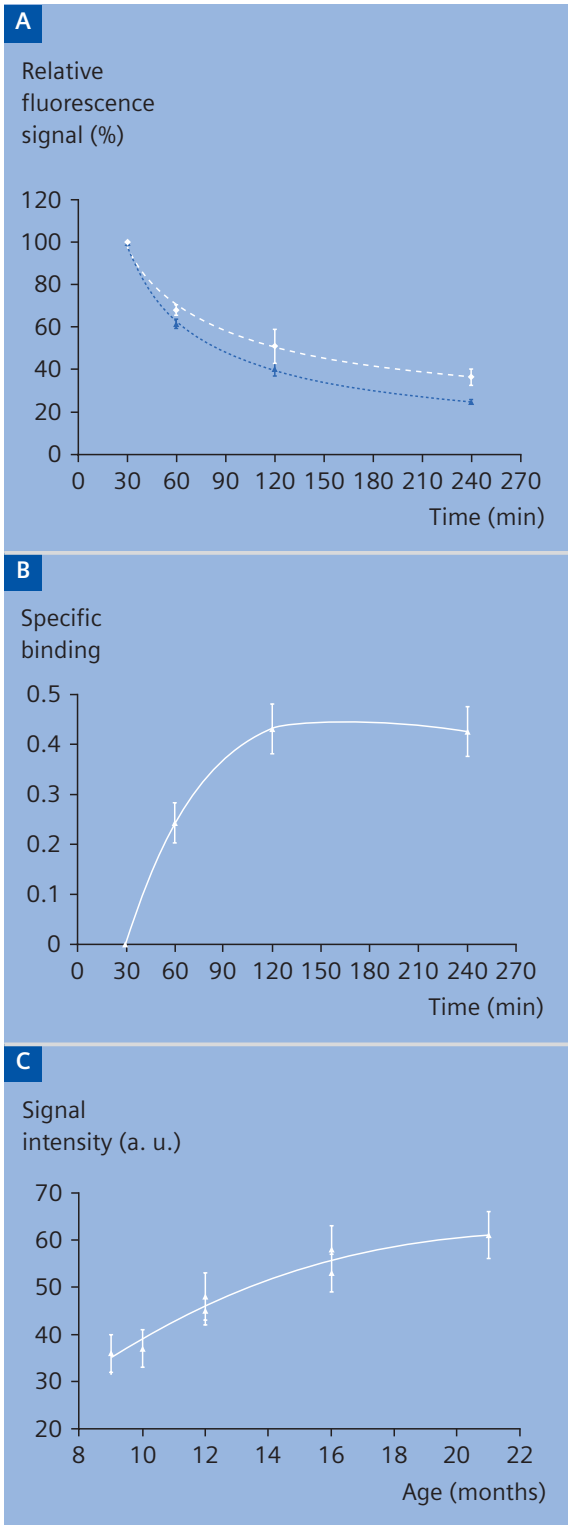


(Figure 3)

Semiquantitative *in vivo* imaging of amyloid- β deposits in living mice

[A] Relative signal activities of 10-month-old APP23 transgenic (upper) and wild-type (lower) mice as a function of time after *i.v.* injection of 0.1 mg/kg AOI987. Statistically significant differences between transgenic and wild-type mice were obtained at the 120- as well as at the 240-minute point ($P = < 0.001$, one-way ANOVA).

[B] Specific binding of AOI987, (i.e., fluorescence signal (transgenic mice) minus fluorescence signal (non-transgenic control mice) divided by fluorescence signal (transgenic mice)), as a function of time after *i.v.* injection of 0.1 mg/kg AOI987 in 16-month-old APP23 mice.

[C] AOI987 fluorescence signal intensity as a function of the age of female APP23 transgenic mice. Each data point represents the mean fluorescence intensity of a set of 10 female APP23 mice of different ages. The corresponding values for age-matched wild-type animals were subtracted to correct for unspecific binding. Two independent measurement series have been collated into the figure illustrating the reproducibility of the measurements. Values are given as mean \pm sem.

the accurate determination of dye distribution and concentration from a single NIRF measurement. Spatial resolution of optical imaging decreases with increasing depth of the fluorescent light source: while microscopic resolution can be achieved when probing superficial structures (or tissue slices), resolution of individual plaques when imaging through the intact cranium and scalp is not feasible. Hence, quantification of the AP load by NIRF imaging is achieved by spatial integration of fluorescence intensities, analogous to the quantification of receptor densities in classic receptor neuroimaging studies.

By normalizing the measured fluorescence reflectance signal intensities to the first imaging time point at 30 minutes after i.v. administration of the dye, we have derived a reliable intensity parameter $I_{\beta}^{rel}(t)$, thereby eliminating unavoidable differences among individual animals. Fluorescence intensity measures for APP23 mice were corrected for the unspecific dye distribution by subtracting the respective intensity values for age-matched wild-type animals. Significant specific binding was observed for APP23 mice of age 9 months and older. The fluorescence intensity and, hence, the extent of specific dye accumulation increased with the age of the animals as expected.

The noninvasiveness of plaque-specific NIRF imaging allows repeated measurements over the life span of a mouse, providing an ideal tool for monitoring progression of AP formation in animal models of AD such as APP23 transgenic mice. The approach is also of high value for evaluation of potential AD drugs in vivo: therapy response can be compared in the same animal to a reference state prior to treatment. Such paired designs should increase the statistical significance of the studies.

Small Animal PET

Compared to optical imaging methods, small animal positron emission tomography (PET) provides clearly superior quantification, high sensitivity, and full three-dimensional information. Today, a number of potential AP-sensitive PET ligands have been developed, some of which are in clinical development [6]. Yet, the obvious methodological advances of small animal PET are counterbalanced by the cost effectiveness of NIRF imaging [8]. Another striking advantage of optical

imaging is the experimental simplicity due to the use of stable dyes: this allows reaching the high throughput numbers required when evaluating potential drug candidates. Therefore, for animal studies, optical techniques offer significant advantages compared to the demands on infrastructure required for PET studies.

Overall, using NIRF imaging, the plaque-specific oxazine dye AOI987 is an attractive probe to noninvasively monitor disease progression in animal models of AD and to evaluate the effectiveness of potential AD drugs.

E/E

For more information, please contact
hansulrich.gremlich@novartis.com

WIP – the information about this product is preliminary. The product is under development and is not commercially available in the U.S., and its future availability cannot be ensured.

References:

- [1] Nussbaum, R. L. & Ellis, C. E. Alzheimer's disease and Parkinson's disease. *New Engl. J. Med.* 348, 1356-1364 [2003].
- [2] Hardy, J. & Selkoe, D. J. The amyloid hypothesis of Alzheimer's disease: progress and problems on the road to therapeutics. *Science* 297, 353-356 [2002].
- [3] Zamrini E., De Santi S. & Tolar M. Imaging is superior to cognitive testing for early diagnosis of Alzheimer's disease. *Neurobiol. Aging* 25, 685-691 [2004].
- [4] Mathis C. A., Wang Y. & Klunk W. E. Imaging β -amyloid plaques and neurofibrillary tangles in the aging human brain. *Curr. Pharm. Design* 10, 1469-1492 [2004].
- [5] Hintersteiner M., Enz A., Frey P., Jaton A.-L., Kinzy W., Kneuer R., Neumann U., Rudin M., Staufienbiel M., Stoeckli M., Wiederhold K.-H. & Gremlich H.-U. In vivo detection of amyloid- β deposits by near-infrared imaging using an oxazine-derivative probe. *Nat. Biotechnol.* 23, 577-583 [2005].
- [6] Klunk W. E., Engler H., Nordberg A., Wang Y., Blomqvist G., Holt D. P., Bergström M., Savitcheva I., Huang G.-F., Estrada S., Ausén B., Debnath M. L., Barletta J., Price J. C., Sandell J., Lopresti B. J., Wall A., Koivisto P., Antoni G., Mathis C. A. & Långström B. Imaging brain amyloid in Alzheimer's disease with Pittsburgh compound-B. *Ann. Neurol.* 55, 306-319 [2004].
- [7] Ntzachristos V., Bremer C. & Weissleder R. Fluorescence imaging with near-infrared light: new technological advances that enable in vivo molecular imaging. *Eur. Radiol.* 13, 195-208 [2003].
- [8] Rudin M. & Weissleder R. Molecular imaging in drug discovery and development. *Nat. Rev.* 2, 123-131 [2003].